Faraday Discussions

Cite this: *Faraday Discuss.*, 2014, **175**, 273



PAPER





# Functionalised gold and titania nanoparticles and surfaces for use as antimicrobial coatings†

Sacha Noimark,[ab] Kristopher Page,[ab] Joseph C. Bear,[a] Carlos Sotelo-Vazquez,[a] Raul Quesada-Cabrera,[a] Yao Lu,[a] Elaine Allan,[b] Jawwad A. Darr[a] and Ivan P. Parkin*[a]

Received 16th May 2014, Accepted 3rd July 2014
DOI: 10.1039/c4fd00113c

We report the preparation, characterisation and antimicrobial functional testing of various titanium dioxide and gold modified titanium dioxide nanoparticles embedded into a polysiloxane polymer by a swell dip-coating procedure. We show that the surfaces are effective in killing both Gram-positive (*Staphylococcus aureus*) and Gram-negative (*Escherichia coli*) bacteria under different lighting conditions. The presence of the nanoparticles was of critical importance in improving the functional properties of the surface. These materials have the potential to reduce hospital-acquired infection, by killing bacteria on the polymer surface.

## 1 Introduction

The prevalence of hospital-acquired infections (HAIs) has been described as 'unacceptably high' by the National Institute for Health and Care Excellence.[1] Each year, approximately 300 000 patients treated at an NHS hospital in England acquire an HAI, including surgical site infections (15.7%), urinary tract infections (17.2%) and infections of the lower respiratory tract or pneumonia (22.8%).[1] An estimated one in 16 patients treated at a U.K. NHS hospital contracts an HAI,[1] with the highest infection rate incidence noted amongst patients in intensive care units.[2] Although interventions have achieved a decrease in the incidence of methicillin-resistant *Staphylococcus aureus* and *Clostridium difficile* infections, the rate of HAIs still poses a significant threat to both healthcare institutions and hospitalised patients.[1]

Hospital touch surfaces act as large reservoirs of bacteria, which can facilitate the spread of infection within healthcare institutions through a surface–

[a]*Materials Chemistry Research Centre, Department of Chemistry, University College London, 20 Gordon St, London, WC1H 0AJ, UK. E-mail: i.p.parkin@ucl.ac.uk; Tel: +44 (0)207 679 4669*
[b]*Division of Microbial Diseases, UCL Eastman Dental Institute, University College London, 256 Grays Inn Road, London, WC1X 8LD, UK*

† Electronic supplementary information (ESI) available. See DOI: 10.1039/c4fd00113c

healthcare worker–patient 'contact' cycle.[3,4] Rigorous hospital cleaning regimes may help reduce hospital surface contamination, however, it is difficult to completely prevent surface contamination or maintain low bacterial loads. One strategy to inhibit the cycle of the transmission of bacteria within a healthcare environment is the utilisation of self-sterilising surfaces. Examples of such surfaces include:[4] microbiocide-releasing surfaces,[5,6] silver and silver doped surfaces,[7,8] copper and copper alloy surfaces,[9–15] and photobactericidal surfaces.[16–32] Microbiocidal surfaces that utilise a light-activated mechanism in which a host of reactive oxygen species are generated are of particular interest, since the non-site specific mode of bacterial attack deems the emergence of bacterial resistance unlikely.[3]

Much research has been invested into the development of photobactericidal polymers activated by laser illumination for use in medical devices.[16–21] Similarly, this technology has also been harnessed for use in antimicrobial surfaces activated by standard hospital white light sources.[22–26] These surfaces were prepared using a simple dipping method, a "swell–encapsulation–shrink" strategy allowing either uniform encapsulation of the light-activated antimicrobial agents throughout the polymer bulk,[16–20,23–26] or both incorporation throughout the polymer bulk in addition to a high concentration at the polymer surface.[21,22] Although laser photo-activated bactericidal surfaces induce the lethal photosensitisation of bacteria in short time periods, laser technology is not practical for use in the sterilisation of touch surfaces commonly found in hospital environments. Conversely, white light-activated antimicrobial surfaces are ideal candidates for applications in general hospital touch surfaces and can help maintain low bacterial surface contamination levels. However, when microbial loads are high, the antimicrobial activity is effective over longer illumination time periods (up to 6 h for *E. coli*[22]). In cases where devices are frequently used and rapid surface sterilisation is preferable, polymers incorporated with UV-activated photocatalytic nanoparticles may prove more suitable.

Titania ($TiO_2$) is used in a wide range of products including white pigment, sunscreens and cosmetics. Inexpensive and robust, $TiO_2$ is an efficient photocatalyst under UV irradiation conditions[33,34] and this well established property has been utilised in applications such as drinking water sterilisation and in self-cleaning windows.[3,35–38] $TiO_2$ has a wide band gap (3.2 eV in the case of anatase $TiO_2$) and therefore requires <385 nm irradiation to activate its photocatalytic properties. The absorption of photons of energy greater than that of the semiconductor band gap results in the promotion of a valance band electron to the semiconductor conduction band. This produces electron–hole pairs, which can interact with adsorbed water and molecular oxygen at the surface of $TiO_2$, forming highly reactive radicals (hydroxyl groups and superoxide ions). These species participate in redox reactions for the degradation of organic pollutants and the killing of bacteria and viruses.[39–41] The mechanism followed in the inhibition of bacterial growth is still unclear, however, it is known that the species photogenerated on the $TiO_2$ surface have an active role in the destruction of the *Escherichia coli* (*E. coli*) cell outer membrane, causing the death of the bacteria.[41–43]

The system formed by $TiO_2$ modified with gold nanoparticles (henceforth Au/$TiO_2$) has been widely studied for environmental applications. These Au/$TiO_2$ systems are potentially efficient as visible-active photocatalysts due to their plasmon induced properties and the improved charge separation (Fermi level

 

shift) which has been proposed previously for similar systems.[44–46] Nevertheless, $Au/TiO_2$ materials have received little attention in antimicrobial applications. Studies involving the sol–gel synthesis of gold-capped $TiO_2$ nanoparticles have shown a beneficial effect of Au-modified $TiO_2$ in the destruction of Gram-negative bacteria (*E. coli*).[47] On the contrary, different observations have been reported for Gram-positive bacteria. Fu *et al.*[47] observed similar inhibition rates in the growth of *Bacillus megaterium* for both $TiO_2$ and $Au/TiO_2$ systems, whereas the antimicrobial activity of the latter was reported to be retarded with respect to pure $TiO_2$ in the killing of *Bacillus subtilis*.[48]

In this paper, we report on the preparation of novel UV-activated photobactericidal polymers by incorporating $TiO_2$ and $Au/TiO_2$ nanoparticles into commercially available medical grade silicone, using a simple dipping technique. The nanoparticles were characterised by Raman, XRD, XPS and TEM and the photocatalytic activities of the $TiO_2$ and $Au/TiO_2$ nanoparticles were compared by investigating the photo-destruction of stearic acid upon UV illumination. The antimicrobial activity of the nanoparticle incorporated polymers was tested against both Gram-negative and Gram-positive bacteria commonly found in healthcare environments and a UVA source (365 nm) was used to activate the photobactericidal properties of these polymers. When tested against *S. aureus*, unprecedented kills were achieved with bacterial numbers reduced to below the detection limit within 15 minutes, without the need for any UV treatment (dark conditions). Although a smaller 'dark kill' effect was noted when tested against *E. coli*, exposure to UV illumination (365 nm) for 95 minutes reduced bacterial numbers to below the detection limit. To our knowledge, this is the first report of the 'dark kill' of bacteria using a titanium dioxide modified polymer. We attribute this kill to the surface functionalisation of the nanoparticles used.

# 2 Experimental

## 2.1 Materials synthesis

**2.1.1 Synthesis of $TiO_2$ nanoparticles.** $TiO_2$ nanoparticles were produced using continuous hydrothermal flow synthesis (CHFS). The pilot scale CHFS system has been described in detail elsewhere.[49,50] Four industrial diaphragm type chemical dosing pumps (Milton Roy, Primeroyal K) carried the precursors under controlled-flow conditions into a confined jet reactor. In the reactor, the precursors were mixed concurrently with supercritical water at 400 °C and 24.1 MPa. The temperature of the system was monitored at different points using type K thermocouples. The actual temperature at the reactor point, in the mixing of supercritical water and the precursor solutions, was 307 °C. Supercritical conditions for the water were reached using a custom built electrical heater arrangement (Watlow Cast X 2000, maximum thermal output 24 kW) and a back-pressure regulator in the system (BPR, Swagelok KHB series), was adjusted using a PID algorithm to maintain pressure. In the synthesis of the $TiO_2$ nanoparticles, each of the precursors, titanium(IV) oxysulfate ($TiOSO_4$ 0.2 M) with free hydrated sulphuric acid (Aldrich) and potassium hydroxide (KOH, 0.4 M) were pumped separately at 150 mL $min^{-1}$ into a T-piece before meeting the flow of supercritical water. The flow rate of supercritical water was adjusted to 300 mL $min^{-1}$. The formed $TiO_2$ nanoparticles were rapidly quenched and cooled using an external cooling system (an outer jacket through which water flowed at 100 L $min^{-1}$ and an

inlet temperature of 15 °C). The nanoparticles were collected as a slurry and subsequently centrifuged and washed three times with deionised water (10 MΩ) until pH neutral and dried in a freeze drier (Virtis Genesis 35XL) by slowly heating from −60 to 25 °C over 24 h under a vacuum of 100 mTorr.

**2.1.2 Deposition of gold nanoparticles on $TiO_2$.** The deposition of gold nanoparticles was carried out following a procedure adapted from the literature.[51] 30 mg of chloroauric acid ($HAuCl_4$), 30 mL of 1% sodium citrate solution and 120 mL of DI water were refluxed for 4 h at 110 °C. 50 mL of the purple Au colloid was then stirred with 1 g of $TiO_2$ nanoparticles and 5.8 g of sodium chloride (NaCl) was suddenly added, resulting in the precipitation of Au metal on the $TiO_2$ particles. The purple precipitate ($Au/TiO_2$) was then filtered, repeatedly washed with deionised water (10 MΩ), centrifuged and lyophilized.

**2.1.3 Functionalisation of $TiO_2$ and $Au/TiO_2$ nanoparticles.** The functionalisation of $TiO_2$ and $Au/TiO_2$ nanoparticles was carried out following a procedure from the literature.[52] $TiO_2$ or $Au/TiO_2$ nanoparticles (1 g) were heated to 80 °C in excess oleic acid (120 mmol, 38.1 mL) over 24 hours, with a catalytic amount of triethylamine (8 mmol, 1.12 mL) added to encourage ester formation between the titanol groups on the particle surfaces and the oleic acid. The nanoparticles were precipitated with ethanol and centrifuged at 2500 *g* before being dispersed in toluene. The nanoparticles were precipitated re-dispersed in toluene three times in order to remove excess surfactant.

**2.1.4 Preparation of antimicrobial polymers.** A series of silicone samples were prepared for microbiological testing. Medical grade silicone polymer coupons (NuSil, Polymer Systems Technology Ltd, 1.21 $cm^2$) were immersed in toluene, oleic acid functionalised $TiO_2$ nanoparticles dispersed in toluene or $Au/TiO_2$ nanoparticles dispersed in toluene, and allowed to swell for 48 h. The samples were subsequently removed from the toluene swelling solutions, air-dried (48 h), washed and towel-dried. Where possible, the samples were maintained under dark conditions. An overview of the materials synthesis is presented in Fig. 1.

## 2.2 Materials characterisation

Transmission electron microscope images were recorded using a Jeol 2100 (high resolution) transmission electron microscope with a $LaB_6$ source operating at an acceleration voltage of 200 kV with an Oxford Instruments XMax EDX detector

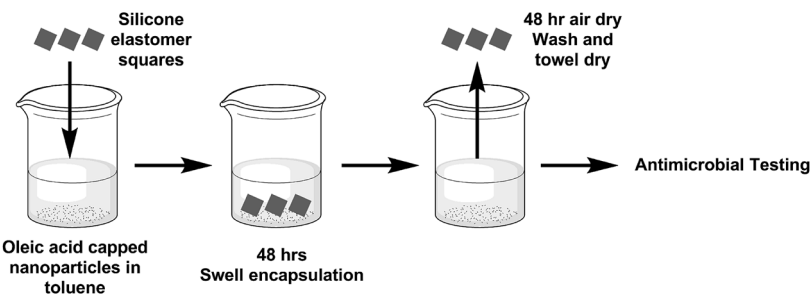


Fig. 1 Schematic to show the preparation of $TiO_2$ and $Au/TiO_2$ encapsulated silicone samples.

 

running AZTEC software. Micrographs were taken using a Gatan Orius Charge-coupled device (CCD). Samples for TEM were prepared by drop-casting a suspension of nanoparticles in hexane solvent onto a 400 Cu mesh holey carbon film TEM grid (Agar Scientific Ltd). UV/Vis spectroscopy was performed using a Perkin Elmer Lambda 950 UV/Vis/NIR spectrophotometer and a PerkinElmer Lambda 25 UV-Vis spectrometer. X-ray diffraction (XRD) data collection was performed using a Bruker-Axs D8 (GADDS) diffractometer. The instrument operates with a Cu X-ray source, monochromated ($K\alpha_1$ and $K\alpha_2$) and a 2D area X-ray detector with a resolution of 0.01°. Films were analysed with a glancing incident angle ($\theta$) of 5°. The diffraction patterns obtained were compared with ICDD database standards. Raman spectra were obtained using a Renishaw Raman System 1000 calibrated using a silicon standard. X-Ray photoelectron spectroscopy (XPS) was performed using a Thermo Scientific K-alpha spectrometer with monochromated Al K$\alpha$ radiation, a dual beam charge compensation system and constant pass energy of 50 eV (spot size 400 μm). Survey scans were collected in the range 0–1200 eV. High-resolution scans were used for the principal peaks of Ti (2p), O (1s), Au (4f) and C (1s), and all spectra were calibrated against adventitious carbon (C1s, 284.8 eV).

### 2.3 Functional properties

**2.3.1 Wetting properties.** Equilibrium water contact angle measurements (~5 μL) were carried out on untreated silicone, solvent treated (control) silicone, unmodified $TiO_2$-encapsulated silicone ($TiO_2$) and gold modified titania-encapsulated silicone ($Au/TiO_2$). The contact angle measurement for each sample type was taken to be the average value over ≥5 measurements, using a droplet of deionised water dispensed by gravity from a gauge 27 needle and the samples were photographed side on. The data was analysed using SURFTENS software (V. 4.5).

**2.3.2 Photocatalytic testing of the $TiO_2$ and $Au/TiO_2$ nanoparticles.** The photo-activity of the nanoparticles was determined by the photo-oxidation of a model organic pollutant, octadecanoic (stearic) acid. In this test, films of $TiO_2$ and $Au/TiO_2$ nanoparticles (0.8 mg) were prepared by drop-casting a concentrated solution of nanoparticles onto borosilicate glass substrates and allowing to dry. A thin layer of stearic acid solution in chloroform (0.05 M) was subsequently dip-coated onto the samples. The samples were irradiated using a blacklight-blue (BLB) lamp (*Vilber Lourmat*, 365 nm) 2 × 8 W, 1.2 mW $cm^{-2}$ and the photo-degradation of the acid was monitored using a Perkin Elmer RX-I Fourier transform infrared (FTIR) spectrometer.

### 2.4 Microbiological testing

The following silicone elastomer samples (1.21 $cm^2$) were used in the microbiology experiments: solvent treated (control), oleic acid functionalised-$TiO_2$-encapsulated ($TiO_2$) and $Au/TiO_2$-encapsulated medical grade silicone. Immediately prior to microbiological testing, all samples were pre-irradiated for 18 hours using a 365 nm UV light source (Vilber Lourmat 365 nm BLB) emitting an average light intensity of 1.8 mW $cm^{-2}$ at a distance of 10 cm from the samples, after which they were maintained under dark conditions (24 h). The samples were subsequently tested against *Staphylococcus aureus* 8325-4 and *Escherichia coli*

ATCC 25922. These organisms were stored at −70 °C in Brain-Heart-Infusion broth (BHI, Oxoid) containing 20% (v/v) glycerol and propagated on either mannitol salt agar (MSA, Oxoid) in the case of *S. aureus*, or MacConkey agar (MAC, Oxoid Ltd.) in the case of *E. coli*, for a maximum of two sub-cultures at intervals of two weeks.

BHI broth (10 mL) was inoculated with 1 bacterial colony and cultured in air at 37 °C for 18 h with shaking at 200 rpm. The bacterial pellet was recovered by centrifugation (21 °C, 1771 × *g*, 5 min), washed in phosphate buffered saline (PBS) and centrifuged again to recover the bacteria, which were finally re-suspended in PBS (10 mL). The washed suspension was diluted 1000-fold to obtain the inoculum (∼106 cfu $mL^{-1}$). The inoculum in each experiment was confirmed by plating ten-fold serial dilutions on agar for viable counts. Triplicates of each polymer sample type were inoculated with 20 μL of the inoculum and covered with a sterile cover slip (22 × 22 mm). The samples were then irradiated for the required time period using a 365 nm UV light source emitting an average light intensity of 1.8 mW $cm^{-2}$ at a distance of 10 cm from the samples. A further set of samples (in triplicate) was maintained in the dark for the duration of the irradiation time.

Post irradiation, the inoculated samples and cover slips were added to PBS (180 μL) and vortexed. The neat suspension and ten-fold serial dilutions were plated on the appropriate agar for viable counts. The plates were incubated aerobically at 37 °C for 24 h (*E. coli*) or 48 h (*S. aureus*). Each experiment contained 3 technical replicates and the experiment was reproduced three times. The Mann–Whitney *U* test was used to determine the significance of the following comparisons: (i) the activity of each of the modified polymers compared to the control silicone sample when both were incubated in the dark and (ii) the activity of each of the irradiated modified polymers compared to the same material incubated in the dark.

# 3 Results and discussion

## 3.1 Materials synthesis and characterisation

Titania nanoparticles were synthesised by continuous hydrothermal flow synthesis (CHFS) and then gold addition was achieved through a modified Turkevich synthesis, which relies upon the gold forming upon the surface of the added titania nanoparticles after precipitation with salt. The titania particles provide a lower energy surface on which gold can grow, rather than undergo Ostwald ripening as they are precipitated. The citrate ligands on the Turkevich gold mean that the nanoparticles are electrostatically stabilised and as such are susceptible to salt flocculation due to a lowering of surface charge. Nanoparticle functionalisation was carried out according to Crick *et al.*,[52] which adds sterically stabilising oleic acid to the surface of the nanoparticles. A portion of the oleic acid is weakly bound (van der Waals interactions) and the rest is esterified with titanol groups on the nanoparticle surfaces.

Silicone samples were embedded with titania and gold–titania nanoparticles using a simple one-step dipping strategy. The modified surfaces were prepared using a "swell–encapsulation–shrink" technique, in which the samples were immersed in a toluene swelling solution made up to 20 mg $mL^{-1}$ nanoparticles for 48 h. The toluene caused significant polymer swelling, enabling the diffusion

 

of the nanoparticles through the polymer bulk. Removal from the swelling solution resulted in polymer shrinkage as residual solvent evaporated. The incorporation of neither the $TiO_2$ nanoparticles nor $Au/TiO_2$ nanoparticles impacted on polymer colouration. This is an attractive property in terms of future commercialisation of this technology for healthcare applications.

The toluene dispersed $TiO_2$ and $Au/TiO_2$ nanoparticle solutions and encapsulated silicone polymers were analysed using UV-Vis absorbance spectroscopy (Fig. 2). The UV-Vis data for the toluene dispersed nanoparticles were used to construct a Tauc plot—$(ahv)^{1/2}$ against energy (eV), where '$a$' is the absorbance of the nanoparticles[29]—to approximate the $TiO_2$ and $Au/TiO_2$ nanoparticle band onset. The data indicate that the presence of gold shifts the band onset of $TiO_2$ towards the visible region of the spectrum (3.18 eV for $Au/TiO_2$ compared to 3.33 eV for $TiO_2$). The UV-Vis absorbance spectra of the $TiO_2$ and $Au/TiO_2$ encapsulated silicone polymers were measured and compared to that of a control silicone polymer. Fig. 2 shows that the band edge of the $TiO_2$ and $Au/TiO_2$-encapsulated silicone polymers is red shifted with respect to that of the control silicone polymer. This provides evidence of polymer nanoparticle encapsulation.

TEM micrographs showed general polydisperse populations of crystalline nanoparticles, dominated by anatase titania in both cases. Nanoparticles were measured to be an average size of $11.2 \pm 4.7$ nm and $10.9 \pm 4.4$ nm for the $TiO_2$ and Au–$TiO_2$ nanoparticle samples respectively, using Image J software. HR-TEM analysis showed highly crystalline samples, with $d$-spacings of *ca.* 0.34 nm and 0.33 nm (Fig. 3(b) and (d)). Using the Bragg equation, both spacings correspond to the $\langle 101 \rangle$ planes of anatase titania. From TEM analysis, nanoparticle size and shape were unaltered by both the gold and oleic acid functionalisation processes. This is possibly due to the small amount of Au (*ca.* 0.36%) being surface bound.

X-Ray diffraction supported the TEM analysis, with broad peaks due to small crystallite sizes compared with bulk anatase $TiO_2$. There was also no discernible change in peak positions on addition of Au. XRD analysis of the polymers

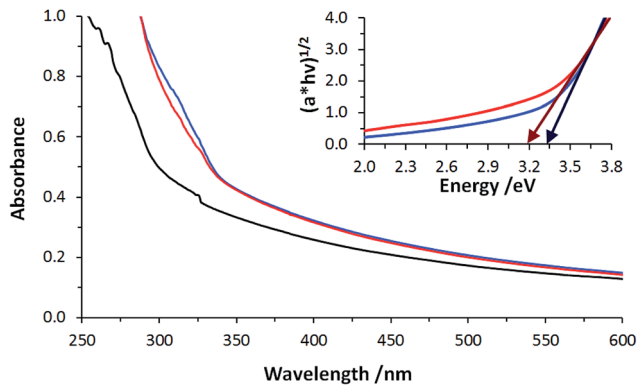


Fig. 2 UV-Vis absorbance spectra of a toluene treated silicone polymer (black line), a $TiO_2$-encapsulated silicone polymer (blue line) and a $Au/TiO_2$-encapsulated silicone polymer (red line). Inset: a Tauc plot to determine the band gap of the $TiO_2$ nanoparticles (blue line) and $Au/TiO_2$ nanoparticles (red line). The band onset of the $TiO_2$ nanoparticles was calculated to be 3.33 eV and the band onset of the $Au/TiO_2$ nanoparticles was calculated to be 3.18 eV.

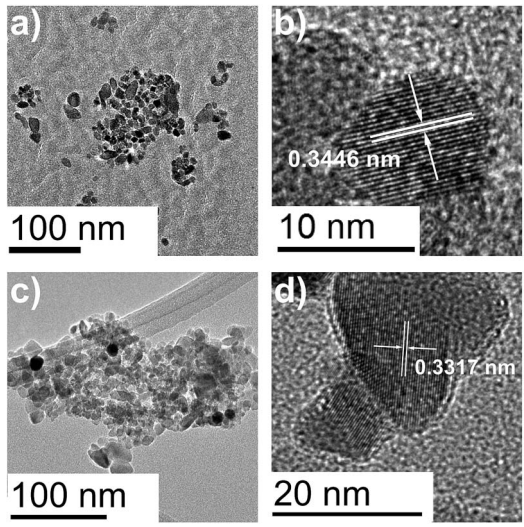


Fig. 3 (a) TEM image of oleic acid functionalised $TiO_2$ nanoparticles, (b) HR-TEM image of oleic acid functionalised $TiO_2$ nanoparticles, (c) TEM image of Au/$TiO_2$ nanoparticles and (d) HR-TEM image of Au/$TiO_2$ nanoparticles.

indicated no difference between the $TiO_2$-encapsulated silicone, Au/$TiO_2$-encapsulated silicone and control silicone. Raman spectra confirmed the anatase structure of the nanoparticles, with visible and characteristic $E_g$, $B_{1g}$ and $A_{1g}$ peaks at 146.7 and 636.7, 396 and 512.5 $cm^{-1}$ for the $TiO_2$-based samples. There was no discernible shift in the Raman peaks between samples and there were no observable characteristic gold peaks (Fig. 4b). Raman spectra of the $TiO_2$- and Au/$TiO_2$-encapsulated silicone both before and after UV irradiation (365 nm, 18 h) were comparable to that of the control silicone sample. This indicates that neither the UV-irradiation, nor the photo-active nanoparticles photo-degrade the silicone polymer. XPS results showed the presence of Au in the Au/$TiO_2$ sample (Fig. 5), albeit in small quantities (*ca.* 0.3%), which is comparable to composition values obtained by EDX. Depth profile studies of the Au/$TiO_2$ powder showed that the gold *vs.* titanium composition did not change throughout the sample, up to a depth of 150 nm (ESI†), suggesting a uniform coating. It is worth noting that there

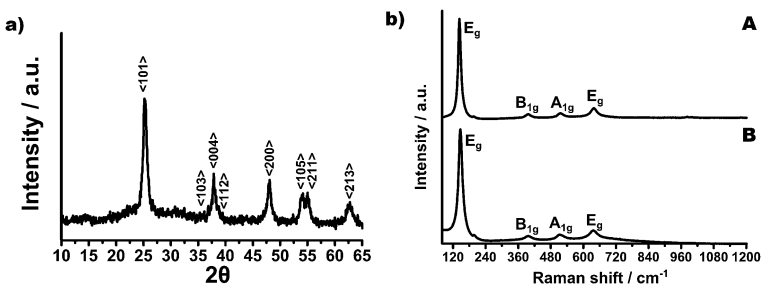


Fig. 4 (a) An X-Ray diffraction pattern of Au/$TiO_2$ showing distinctive peaks of anatase $TiO_2$ and (b) Raman spectra of the $TiO_2$ and Au/$TiO_2$ samples.[53]

is no discernible shift in the binding energies and chemical environments of the Ti 2p and O 1s in the two samples. XPS and EDX elemental composition information is available in the ESI.†

### 3.2 Functional properties

The wetting properties of a range of untreated and treated silicone samples were measured under the laboratory temperature and lighting conditions. The measurements indicated that the polymer itself is highly hydrophobic (120°) and the water contact angle is reduced upon encapsulation of the $TiO_2$ and $Au/TiO_2$ nanoparticles (90°). No photo-induced polymer hydrophilicity was observed upon incorporation of the nanoparticles. It can be speculated that this is because the nanoparticles do not form a thin film at the polymer surface, rather they are dispersed throughout the polymer matrix and therefore impact on the hydrophilicity of the polymer, rather than the UV-activated hydrophilicity.

The photoactivity of the films was evaluated during photodegradation of stearic acid, a model organic pollutant. Stearic acid is highly stable under UV irradiation in the absence of an underlying, effective photocatalyst film. The overall oxidation reaction is given by eqn (1) and it is monitored for transparent samples by infrared spectroscopy, following the disappearance of typical C–H bands at 2958, 2923 and 2853 $cm^{-1}$ (Fig. 6a).

$$CH_3(CH_2)_{16}CO_2H + 26O_2 \xrightarrow{TiO_2(h\nu) \geq E_{bg}} 18CO_2 + 18H_2O \quad (1)$$

The number of acid molecules degraded is estimated using a conversion factor from the literature[54] (1 $cm^{-1} = 9.7 \times 10^{15}$ molecules per $cm^2$). The photoactivity rates are estimated from linear regression of the initial 20–30% degradation steps (zero-order kinetics regime) of the curves of integrated areas (Fig. 6b).

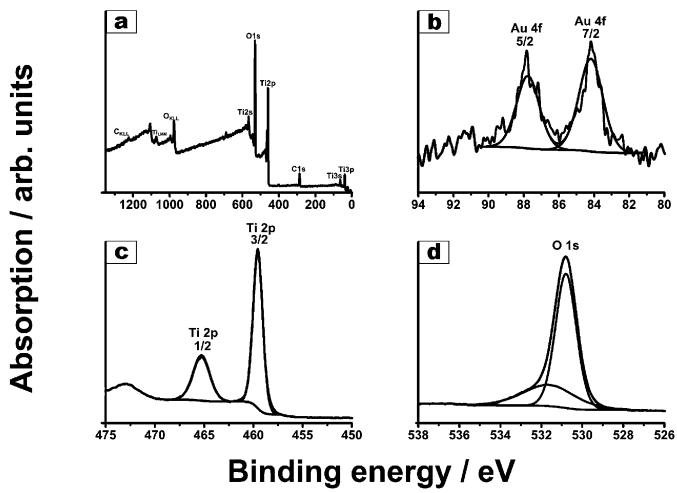


Fig. 5 Fitted XPS spectra of $Au/TiO_2$. (a) Labelled survey scan, (b) Au 4f scan, (c) Ti 2p scan and (d) O 1s scan.

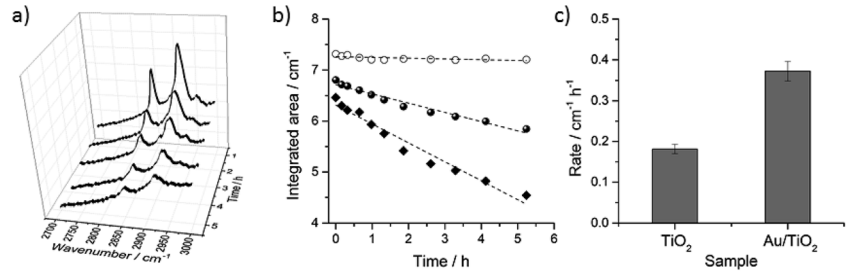


Fig. 6 (a) IR spectra of stearic acid upon UVA illumination (1.2 mW cm$^{-2}$) on a $TiO_2$ drop-cast film. (b) Integrated areas obtained during illumination of $TiO_2$ (full circles), Au/$TiO_2$ (full diamonds) and plain glass control (open circles) films. (c) Photo-activity rates (given as rate over irradiance) of $TiO_2$ and Au/$TiO_2$ films obtained during UVA irradiation (BLB 365 nm).

Preliminary photocatalytic tests of drop-cast films of $TiO_2$ and Au/$TiO_2$ powders showed an enhanced activity in the case of the latter material (Fig. 6c), in agreement with the literature.[54] The enhanced activity of $TiO_2$-based systems containing noble metal nanoparticles is typically explained in terms of an efficient charge separation as shown in Fig. 7.

### 3.3 Photobactericidal activity

We report the light-activated antimicrobial activity of titania nanoparticle encapsulated silicone sample systems when tested against representative Gram-positive and Gram-negative bacteria, *S. aureus* and *E. coli* respectively, both of which are commonly found in healthcare environments. The samples were

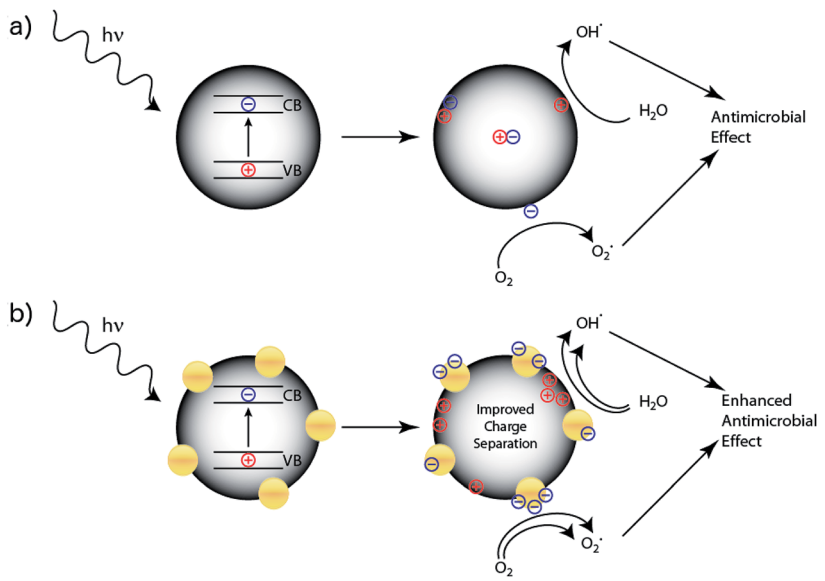


Fig. 7 Proposed mechanism of photocatalytic antimicrobial activity of (a) the $TiO_2$ encapsulated silicone sample and (b) the Au/$TiO_2$ encapsulated silicone sample.

 

pre-irradiated (18 h) with a 365 nm UV lamp prior to testing to photodegrade residual organic precursor material, after which they were stored under dark conditions (24 h). In each experiment the samples were irradiated with a 365 nm UV lamp emitting an average of 1.8 mW $cm^{-2}$ at a distance of 10 cm, whilst a control sample set was maintained under dark conditions for the same duration, to determine whether bacterial kills are attributed to a photocatalysed effect or intrinsic bactericidal properties of the surfaces.

The antimicrobial activity of medical grade silicone encapsulated with $TiO_2$ or $Au/TiO_2$ nanoparticles was compared to that of a control, solvent treated silicone sample. Interestingly, when tested against *S. aureus*, both titania incorporated samples demonstrated potent bactericidal activity under dark conditions, with bacterial numbers reduced to below the detection limit ($P < 0.001$, Fig. 8a). As a result, no additional photosensitisation effects could be determined. $TiO_2$ is a photo-activated antimicrobial agent and thus, it was surprising to observe bactericidal activity under dark conditions. Hence, it can be speculated that the exhibited antimicrobial properties of the $TiO_2$ and $Au/TiO_2$ encapsulated polymers can be attributed to the oleic acid capping agent on the nanoparticles, which has been noted to inhibit growth of Gram-positive bacteria including *S. aureus*.[55] Further experiments with different oleic acid capped nanoparticles would be of benefit in elucidating the mechanism of 'dark kill' observed in this study.

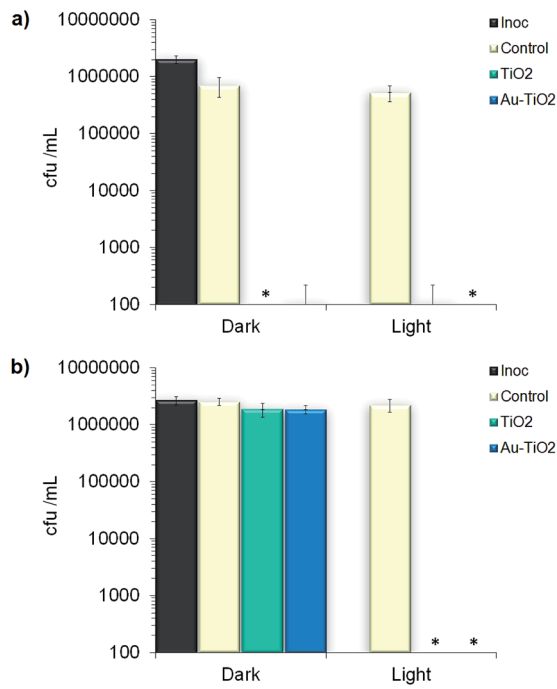


Fig. 8 Viable counts of bacteria (colony forming units (cfu) per mL) after incubation on modified silicone polymers exposed to UV irradiation (365 nm): (a) *S. aureus* (15 min illumination) and (b) *E. coli* (95 min illumination). The UV source emitted an average light intensity of $1.8 \pm 0.1$ mW $cm^{-2}$ at a distance of 10 cm from the samples. * symbols indicate that the bacterial numbers were reduced to below the detection limit of 500 cfu $mL^{-1}$.

Fig. 8b shows that under dark conditions, both the $TiO_2$-encapsulated silicone and the Au/$TiO_2$-encapsulated silicone exhibited limited antimicrobial activity against *E. coli*, although these effects were not highly significant ($P < 0.01$). This observation indicates that the bactericidal properties of the capping agent are not as effective against this bacterium. However, the data show that when exposed to a 365 nm UV lamp, both the $TiO_2$ and Au/$TiO_2$ samples exhibited efficacious photo-activated properties, reducing viable bacterial numbers to below the detection limit within 95 minutes ($P < 0.001$).

$TiO_2$, a UV-activated photocatalyst, generates electron–hole pairs upon absorption of photons with energy greater than that of its band gap energy. The electrons can interact with molecular oxygen in the vicinity generating superoxide anions, whereas the positive holes at the nanoparticle surface can interact with adsorbed water, generating hydroxyl radicals. The photo-generated radical species can subsequently react further, resulting in the production of a wide range of radicals. These radicals can initiate a multi-site attack against bacteria in the environs, oxidising organic matter and subsequently photo-destroying bacterial cellular membranes and components. Due to the non-site specific attack mechanism, the emergence of bacterial resistance is highly unlikely. This is a highly desirable property in antimicrobial surfaces developed for applications in healthcare settings.

In this study, it was not possible to determine whether the presence of Au enhanced the photo-activity of the $TiO_2$ nanoparticles. However, rapid kills were achieved on both the $TiO_2$ and Au/$TiO_2$ samples when tested against *S. aureus* and *E. coli*, with viable bacterial numbers reduced to below the detection limit. Further microbial investigations involving white light activation or shorter illumination times may shed light onto whether the Au shifts the nanosized $TiO_2$ towards visible light photocatalysis or improves the antimicrobial efficacy over that of $TiO_2$ alone. Moreover, microbial testing on surfaces incorporated with a range of oleic acid-capped nanoparticles may be of interest. It would also be advantageous in further investigations to study organisms with known antibiotic resistance or recent clinical isolates.

# 4 Conclusion

We report a new class of potent UV-activated antimicrobial polymers by incorporating nano-$TiO_2$ and nano-Au/$TiO_2$ into medical grade silicone. These surfaces induced the lethal photosensitisation of *E. coli* within 95 minutes, with bacterial numbers reduced to below the detection limit. They also exhibited efficacious antimicrobial activity against *S. aureus via* a non-light-activated mechanism, reducing bacterial numbers to below the detection limit within 15 minutes. The incorporation of nanoparticles did not affect polymer colouration, a highly desirable property from a commercial viewpoint.

# Acknowledgements

The authors would like to thank the EPSRC for their financial support. IPP and SN would also like to thank Ondine Biomedical for their financial support. The authors would like to thank Mr Martin Vickers for assistance in XRD, Dr Robert

 

Palgrave for assistance in XPS and Dr Steven Firth for assistance in TEM and Raman.



## References

1 Doctors and nurses must redouble hygiene efforts to bring down 'unacceptable and avoidable' infection rates, http://http://www.nice.org.uk/newsroom/pressreleases/DoctorsAndNursesMustRedouble\\HygieneEffortsToBringDownInfectionRates.jsp, accessed: 27-04-2014.
2 HCAI and Antimicrobial Point Prevalence Survey England, http://www.hpa.org.uk/Topics/InfectiousDiseases/InfectionsAZ/HCAI/HCAIPointPrevalenceSurvey/, accessed: 27-04-2014.
3 S. Noimark, C. W. Dunnill and I. P. Parkin, *Adv. Drug Delivery Rev.*, 2013, **65**, 570–580.
4 K. Page, M. Wilson and I. P. Parkin, *J. Mater. Chem.*, 2009, **19**, 3819–3831.
5 C. E. Edmiston, F. C. Daoud and D. Leaper, *Surgery*, 2013, **154**, 89–100.
6 D. L. Williams, K. D. Sinclair, S. Jeyapalina and R. D. Bloebaum, *J. Biomed. Mater. Res., Part B*, 2013, **101**, 1078–1089.
7 AcryMed Inc., SilvaGardTM Technology Summary., http://www.acrymed.com/pdf/SilvaGard%20Technical%20Summary.pdf, accessed: 2013-07-22.
8 AgION Technologies Inc., AgIONTM Technology, http://www.agion-tech.com, accessed: 2013-07-22.
9 F. Marais, S. Mehtar and L. Chalkley, *J. Hosp. Infect.*, 2010, **74**, 80–82.
10 S. A. Wilks, H. Michels and C. W. Keevil, *Int. J. Food Microbiol.*, 2005, **105**, 445–454.
11 T. J. Karpanen, A. L. Casey, P. A. Lambert, B. D. Cookson, P. Nightingale, L. Miruszenko and T. S. J. Elliott, *Infect. Control Hosp. Epidemiol.*, 2012, **33**, 3–9.
12 C. D. Salgado, K. A. Sepkowitz, J. F. John, J. R. Cantey, H. H. Attaway, K. D. Freeman, P. A. Sharpe, H. T. Michels and M. G. Schmidt, *Infect. Control Hosp. Epidemiol.*, 2013, **34**, 479–486.
13 J. O. Noyce, H. Michels and C. W. Keevil, *J. Hosp. Infect.*, 2006, **63**, 289–297.
14 L. Weaver, H. T. Michels and C. W. Keevil, *J. Hosp. Infect.*, 2008, **68**, 145–151.
15 M. G. Schmidt, H. H. Attaway, P. A. Sharpe, J. John, K. A. Sepkowitz, A. Morgan, S. E. Fairey, S. Singh, L. L. Steed, J. R. Cantey, K. D. Freeman, H. T. Michels and C. D. Salgado, *J. Clin. Microbiol.*, 2012, **50**, 2217–2223.
16 S. Perni, C. Piccirillo, J. Pratten, P. Prokopovich, W. Chrzanowski, I. P. Parkin and M. Wilson, *Biomaterials*, 2009, **30**, 89–93.
17 S. Perni, C. Piccirillo, A. Kafizas, M. Uppal, J. Pratten, M. Wilson and I. P. Parkin, *J. Cluster Sci.*, 2010, **21**, 427–438.
18 S. Perni, P. Prokopovich, C. Piccirillo, J. Pratten, I. P. Parkin and M. Wilson, *J. Mater. Chem.*, 2009, **19**, 2715–2723.
19 S. Perni, J. Pratten, M. Wilson, C. Piccirillo, I. P. Parkin and P. Prokopovich, *J. Biomater. Appl.*, 2011, **25**, 387–400.
20 S. Noimark, C. W. Dunnill, C. W. M. Kay, S. Perni, P. Prokopovich, S. Ismail, M. Wilson and I. P. Parkin, *J. Mater. Chem.*, 2012, **22**, 15388–15396.
21 S. Noimark, M. Bovis, A. J. MacRobert, A. Correia, E. Allan, M. Wilson and I. P. Parkin, *RSC Adv.*, 2013, **3**, 18383–18394.
22 S. Noimark, E. Allan and I. P. Parkin, *Chem. Sci.*, 2014, **5**, 2216–2223.

23 A. J. T. Naik, S. Ismail, C. Kay, M. Wilson and I. P. Parkin, *Mater. Chem. Phys.*, 2011, **129**, 446–450.
24 V. Decraene, J. Pratten and M. Wilson, *Appl. Environ. Microbiol.*, 2006, **72**, 4436–4439.
25 V. Decraene, J. Pratten and M. Wilson, *Curr. Microbiol.*, 2008, **57**, 269–273.
26 M. Wilson, *Infect. Control Hosp. Epidemiol.*, 2003, **24**, 782–784.
27 J. Bozja, J. Sherrill, S. Michielsen and I. Stojiljkovic, *J. Polym. Sci., Part A: Polym. Chem.*, 2003, **41**, 2297–2303.
28 M. Wainwright, M. N. Byrne and M. A. Gattrell, *J. Photochem. Photobiol., B*, 2006, **84**, 227–230.
29 C. W. Dunnill, K. Page, Z. A. Aiken, S. Noimark, G. Hyett, A. Kafizas, J. Pratten, M. Wilson and I. P. Parkin, *J. Photochem. Photobiol., A*, 2011, **220**, 113–123.
30 Z. A. Aiken, G. Hyett, C. W. Dunnill, M. Wilson, J. Pratten and I. P. Parkin, *Chem. Vap. Deposition*, 2010, **16**, 19–22.
31 C. W. Dunnill, Z. Ansari, A. Kafizas, S. Perni, D. J. Morgan, M. Wilson and I. P. Parkin, *J. Mater. Chem.*, 2011, **21**, 11854–11861.
32 C. W. Dunnill, Z. A. Aiken, J. Pratten, M. Wilson and I. P. Parkin, *Chem. Vap. Deposition*, 2010, **16**, 50–54.
33 A. Mills and S. LeHunte, *J. Photochem. Photobiol., A*, 1997, **108**, 1–35.
34 M. R. Hoffmann, S. T. Martin, W. Y. Choi and D. W. Bahnemann, *Chem. Rev.*, 1995, **95**, 69–96.
35 A. Mills, R. H. Davies and D. Worsley, *Chem. Soc. Rev.*, 1993, **22**, 417–425.
36 A. Mills, N. Elliott, I. P. Parkin, S. A. O'Neill and R. J. H. Clark, *J. Photochem. Photobiol., A*, 2002, **151**, 171–179.
37 S. A. O'Neill, I. P. Parkin, R. J. H. Clark, A. Mills and N. Elliott, *J. Mater. Chem.*, 2003, **13**, 56–60.
38 A. Mills, G. Hill, M. Crow and S. Hodgen, *J. Appl. Electrochem.*, 2005, **35**, 641–653.
39 J. C. Yu, W. K. Ho, J. Lin, K. Y. Yip and P. K. Wong, *Environ. Sci. Technol.*, 2003, **37**, 2296–2301.
40 L. K. Adams, D. Y. Lyon and P. J. J. Alvarez, *Water Res.*, 2006, **40**, 3527–3532.
41 K. Sunada, Y. Kikuchi, K. Hashimoto and A. Fujishima, *Environ. Sci. Technol.*, 1998, **32**, 726–728.
42 D. M. Blake, P. C. Maness, Z. Huang, E. J. Wolfrum, J. Huang and W. A. Jacoby, *Sep. Purif. Methods*, 1999, **28**, 1–50.
43 Z. X. Lu, L. Zhou, Z. L. Zhang, W. L. Shi, Z. X. Xie, H. Y. Xie, D. W. Pang and P. Shen, *Langmuir*, 2003, **19**, 8765–8768.
44 Y. Tian and T. Tatsuma, *J. Am. Chem. Soc.*, 2005, **127**, 7632–7637.
45 K. Kimura, S.-i. Naya, Y. Jin-nouchi and H. Tada, *J. Phys. Chem. C*, 2012, **116**, 7111–7117.
46 M. J. Uddin, F. Cesano, D. Scarano, F. Bonino, G. Agostini, G. Spoto, S. Bordiga and A. Zecchina, *J. Photochem. Photobiol., A*, 2008, **199**, 64–72.
47 G. F. Fu, P. S. Vary and C. T. Lin, *J. Phys. Chem. B*, 2005, **109**, 8889–8898.
48 L. Armelao, D. Barreca, G. Bottaro, A. Gasparotto, C. Maccato, C. Maragno, E. Tondello, U. L. Stangar, M. Bergant and D. Mahne, *Nanotechnology*, 2007, **18**, 375709.
49 C. J. Tighe, R. I. Gruar, C. Y. Ma, T. Mahmud, X. Z. Wang and J. A. Darr, *J. Supercrit. Fluids*, 2012, **62**, 165–172.
50 R. I. Gruar, C. J. Tighe and J. A. Darr, *Ind. Eng. Chem. Res.*, 2013, **52**, 5270–5281.

 

51 A. Mills, *J. Chem. Soc., Chem. Commun.*, 1982, 367–368.
52 C. R. Crick, J. C. Bear, A. Kafizas and I. P. Parkin, *Adv. Mater.*, 2012, **24**, 3505–3508.
53 W. F. Zhang, Y. L. He, M. S. Zhang, Z. Yin and Q. Chen, *J. Phys. D: Appl. Phys.*, 2000, **33**, 912–916.
54 A. Mills and J. Wang, *J. Photochem. Photobiol., A*, 2006, **182**, 181–186.
55 F. Dilika, P. D. Bremner and J. J. Meyer, *Fitoterapia*, 2000, **71**, 450–452.